Notch inhibition overcomes resistance to tyrosine kinase inhibitors in EGFR-driven lung adenocarcinoma

Emilie Bousquet Mur, Sara Bernardo, Laura Papon, Maicol Mancini, Eric Fabbrizio, Marion Goussard, Irene Ferrer, Anais Giry, Xavier Quantin, Jean-Louis Pujol, et al.

Notch inhibition overcomes resistance to tyrosine kinase inhibitors in EGFR-driven lung adenocarcinoma

Emilie Bousquet Mur[1], Sara Bernardo[1], Laura Papon[1], Maicol Mancini[1], Eric Fabbrizio[1], Marion Goussard[1], Irene Ferrer[1, 2, 3], Anais Giry[1], Xavier Quantin[1], Jean-Louis Pujol[1, 4], Olivier Calvayrac[5], Herwig P. Moll[6], Yaël Glasson[7], Nelly Pirot[7], Andrei Turtoi[8], Marta Cañamero[9], Kwok-Kin Wong[10], Yosef Yarden[11], Emilio Casanova[6, 12], Jean-Charles Soria[13], Jacques Colinge[14], Christian W. Siebel[15], Julien Mazieres[5, 16], Gilles Favre[5], Luis Paz-Ares[2, 4, 17], Antonio Maraver[1,*]

[1] *Oncogenic pathways in lung cancer, Institut de Recherche en Cancérologie de Montpellier (IRCM), Univ Montpellier, Institut Régional du Cancer de Montpellier (ICM), Montpellier, 34298, Cedex 5, France.*
[2] *Unidad de Investigación Clínica de Cáncer de Pulmón, Instituto de Investigación Hospital 12 de Octubre-CNIO, Madrid, 28029-28041, Spain.*
[3] *CIBERONC, 28029, Madrid, Spain.*
[4] *Montpellier Academic Hospital, Hôpital Arnaud de Villeneuve, 34090, Cedex 5, Montpellier, France.*
[5] *Inserm, Centre de Recherche en Cancérologie de Toulouse, CRCT UMR-1037, Toulouse, France; Institut Claudius Regaud, IUCT-Oncopole, Laboratoire de Biologie Médicale Oncologique, Toulouse, France; University of Toulouse III (Paul Sabatier), Toulouse, France.*
[6] *Department of Physiology, Center of Physiology and Pharmacology and Comprehensive Cancer Center (CCC), Medical University of Vienna, AT-1090 Vienna, Austria*
[7] *Réseau d'Histologie Expérimentale de Montpellier, BioCampus, UMS3426 CNRS-US009 INSERM-UM, Montpellier, France.*
[8] *Tumor microenvironment and resistance to treatment, Institut de Recherche en Cancérologie de Montpellier (IRCM), Univ Montpellier, Institut Régional du Cancer de Montpellier (ICM), Montpellier, 34298, Cedex 5, France.*
[9] *Roche Pharmaceutical Research and Early Development, Translational Medicine, Roche Innovation Center, Munich, Germany.*
[10] *Laura and Isaac Perlmutter Cancer Center, NYU Langone Medical Center, New York, NY 10016, USA.*
[11] *Department of Biological Regulation, Weizmann Institute of Science, Rehovot, 76100, Israel.*
[12] *Ludwig Boltzmann Institute for Cancer Research (LBI-CR), Vienna 1090, Austria.*
[13] *Drug Development Department (DITEP), Gustave Roussy Cancer Campus, Paris-Sud University, Villejuif, 76100, France*
[14] *Cancer bioinformatics and systems biology, Institut de Recherche en Cancérologie de Montpellier (IRCM), Univ Montpellier, Institut Régional du Cancer de Montpellier (ICM), Montpellier, 34298, Cedex 5, France.*
[15] *Department of Discovery Oncology, Genentech, Inc., 1 DNA Way, South San Francisco, CA 94080, USA.*
[16] *Thoracic Oncology Department, Larrey Hospital, University Hospital of Toulouse, France; Inserm, Centre de Recherche en Cancérologie de Toulouse, CRCT UMR-1037, Toulouse, France; University of Toulouse III (Paul Sabatier), Toulouse, France.*
[17] *Medical School, Universidad Complutense, 28040, Madrid, Spain.*

Conflict of interest statement: The authors have declared that no conflict of interest exists.

Correspondence to:

Antonio Maraver, PhD
Oncogenic pathways in lung cancer
Institut de Recherche en Cancérologie de Montpellier
Inserm U1194 - Université Montpellier - ICM
Campus Val d'Aurelle
208 Rue des Apothicaires
F-34298 Montpellier Cedex 5, France
Tel office: +33(0) 467 612 395
Fax: +33(0) 467 613 787
e-mail: antonio.maraver@inserm.fr

ABSTRACT

EGFR mutated lung adenocarcinoma patients treated with gefitinib and osimertinib showed a therapeutic benefit limited by the appearance of secondary mutations, such as $EGFR^{T790M}$ and $EGFR^{C797S}$. It is generally thought that these secondary mutations render EGFR completely unresponsive to such inhibitors. Here, we found that gefitinib and osimertinib increased STAT3 phosphorylation (pSTAT3) in lung adenocarcinoma cells harboring the $EGFR^{T790M}$ and the $EGFR^{C797S}$ mutations. Moreover, concomitant treatment with a Notch inhibitor and gefitinib or osimertinib strongly reduced the expression of the transcriptional repressor HES1, in a pSTAT3-dependent manner. Importantly, we show that tyrosine kinase inhibitor resistant tumors, with $EGFR^{T790M}$ and $EGFR^{C797S}$ mutations, are highly responsive to treatment with the combination of Notch inhibitors and gefitinib or osimertinib, respectively. Finally, in patients with lung adenocarcinoma harboring EGFR mutations treated with tyrosine kinase inhibitors, HES1 protein levels increased during relapse, and high HES1 expression level correlated with shorter progression-free survival. Our results offer a proof of concept for a novel alternative to treat patients with lung adenocarcinoma after disease progression following osimertinib treatment.

INTRODUCTION

Lung cancer kills about a million people every year worldwide being the leading cause of death by cancer in the world. There are two main types of lung cancer: small cell lung carcinoma (about 20% of all lung cancers) and non-small-cell lung carcinoma that includes lung adenocarcinoma (40%), lung squamous carcinoma (30%), and large cell carcinoma (about 10% of all lung cancers) (1). *EGFR* gene alterations are detected in about 20% of patients with lung adenocarcinoma in Western countries, and in up to 50% in some Asian countries, such as Korea. The most common EGFR alterations in lung adenocarcinoma are exon 19 deletion and the activating $EGFR^{L858R}$ mutation (2). The life expectancy of patients has improved dramatically thanks to the development of EGFR tyrosine kinase inhibitors (TKI) (3). Most of the patients treated with first-generation TKIs (i.e., gefitinib and erlotinib) initially respond well; however, their tumors rapidly develop resistance. This is explained, in about 60% of cases, by acquisition of the so-called 'gatekeeper' mutation $EGFR^{T790M}$ (4). More recently, third-generation TKIs that target $EGFR^{T790M}$, such as osimertinib, have shown a very good therapeutic effect in patients with this mutation (5). Unfortunately, tumors from patients treated with osimertinib also become resistant to this drug. In about 30% of cases, this is due to appearance of new gatekeeper mutations, such as $EGFR^{C797S}$ (6, 7). Thus, treatment of EGFR-driven lung adenocarcinoma with a single TKI might have limited value, and strategies based on combinational drug therapies could be more effective for controlling the effects of gatekeeper mutations.

The $EGFR^{T790M}$ gatekeeper mutation confers resistance to TKIs through different mechanisms, such as weaker drug binding due to steric hindrance and increased ATP affinity of mutated EGFR (8). However, gefitinib binding to $EGFR^{T790}$ protein is reduced, but not totally inhibited (8). Moreover, X-ray structure analysis indicates that

gefitinib binds in a similar manner to wild type EGFR and to $EGFR^{T790M}$ proteins (9). Therefore, we hypothesized that in tumors with gatekeeper EGFR mutations, gefitinib could still affect EGFR downstream signaling pathways, although not reaching therapeutic effect, and that this could be exploited by concomitantly inhibiting other signaling pathways.

The Notch signaling pathway is highly conserved among metazoans, and it is important during embryonic development as well as adult tissue homeostasis. In mammals, there are four NOTCH receptors (NOTCH1 to 4) that are activated upon interaction with their transmembrane ligands (DELTA and JAGGED). For this activation to occur, an intramembrane protease called γ-secretase, releases the Notch intracytoplasmic domain (NICD). Upon nuclear translocation and binding to its DNA binding partner RBPJ, NICD modulates the expression of target genes of the canonical Notch pathway, such as HES1 (10). Therefore, the Notch pathway can be inhibited by γ-secretase inhibitors (GSIs), or by antibodies against the Notch ligands and receptors (11).

By making use of genetically engineered mouse models, we and others demonstrated that KRAS-driven lung adenocarcinoma is dependent on Notch activity (12-14). Moreover, seminal *in vitro* and *in vivo* (mouse xenografts) studies using lung cancer cell lines showed that the combination of Notch inhibitors and EGFR TKIs gives a better anti-tumor response than single treatments in sensitive cells (15-17). However, the underlying mechanism is not fully understood, and the role of the Notch pathway in lung adenocarcinoma after relapse due to acquisition of gatekeeper mutations in EGFR remains largely unknown.

Here, to find some answers to these questions, we first performed a transcriptomic analysis in human lung adenocarcinoma PC9GR cells harboring the $EGFR^{T790M}$

gatekeeper mutation, and found that after gefitinib treatment, several pathways, including the KRAS signaling pathway, were downregulated. Therefore, based on our previous results concerning the importance of Notch in KRAS-driven lung adenocarcinoma (14), we tested the combined effect of TKI and Notch inhibition in different preclinical mouse models of lung adenocarcinoma with the $EGFR^{T790M/L858R}$ mutations. We found that *in vivo* Notch inhibition overcame resistance to gefitinib in human and murine lung adenocarcinoma cells via pSTAT3 binding to the *HES1* promoter and HES1 decreased expression. Similarly, Notch inhibition re-sensitized also *in vivo* human lung adenocarcinoma cells harboring the $EGFR^{C797S}$ mutation, that cause resistance to osimertinib, which might become soon the first-line treatment for patients with EGFR-driven lung adenocarcinoma. Altogether, our data show that concomitant Notch inhibition with TKI, could be a potent strategy to treat EGFR-driven lung adenocarcinoma patients after TKI relapse.

RESULTS

Gefitinib treatment in human lung adenocarcinoma cells with the gatekeeper mutation *EGFR^{T790M}* induces changes in several cancer-associated genetic signatures

To identify molecular changes upon gefitinib treatment in lung cancer cells harboring the *EGFR^{T790M}* mutation that confers resistance to first-generation TKIs, we used the already described human EGFR-driven lung adenocarcinoma PC9GR cell line (*EGFR^{T790M}*) resistant to gefitinib (18). Gene set enrichment analysis using the «Molecular Signatures Database Hallmark Gene Set Collection» (19, 20) of data obtained by RNA-seq of PC9GR cells treated with vehicle or gefitinib showed that among the fifty signatures, only one was upregulated (HALLMARK_KRAS_SIGNALING_DN) (Supplemental Table 1). Accordingly, among the eight downregulated gene sets in gefitinib-treated cells, we found "HALLMARK_KRAS_SIGNALING_UP" (Figure 1A and Supplemental Table 1). This suggests that in PC9GR cells, gefitinib decreases the activity of the KRAS signaling pathway, a well-known EGFR downstream pathway (21).

We previously reported that the Notch pathway plays a major role in KRAS-driven lung adenocarcinoma, and that its inhibition fully stops tumor growth in this setting (14). Therefore, we hypothesized that gefitinib effects in PC9GR cells harboring the *EGFR^{T790M}* gatekeeper mutation could be enhanced by Notch inhibition.

Inhibition of Notch signaling hampers tumor growth in *EGFR$^{T790M/L858R}$* mice

Before directly testing this hypothesis, we studied the Notch pathway activation in EGFR-driven lung tumors *in vivo*, by crossing *EGFR$^{T790M/L858R}$* (22) and lung-specific *CCSP-rtTA* transgenic mice (23) to obtain mice in which *EGFR$^{T790M/L858R}$* expression in

lungs can be induced by treatment with doxycycline (*EGFR*$^{T790M/L858R}$ mice, hereafter). After 8 weeks of doxycycline treatment, mice developed bronchial and peripheral *EGFR*$^{T790M/L858R}$-driven tumors that are resistant to first-generation EGFR TKIs, such as gefitinib (22). Western blot analysis showed that N1ICD, the processed and active form of NOTCH1, and HES1, a Notch target gene, were strongly expressed in *EGFR*$^{T790M/L858R}$-driven tumors compared with normal lung tissue from control mice (either littermates with the same genotype but not treated with doxycycline, or CCSP-rtTA transgenic mice treated with doxycycline) (Figure 1B). This finding is similar to what observed in the *Kras*^{G12V} mouse model (14), and suggests that the Notch pathway may play a similar role in both tumor types.

As the NOTCH1 and NOTCH3 receptors promote *Kras*^{G12V}-driven lung adenocarcinoma, whereas NOTCH2 has a tumor suppressive role (12, 13, 24), we analyzed their expression in *EGFR*$^{T790M/L858R}$-driven lung adenocarcinoma. The transmembrane forms of NOTCH1 and NOTCH3 (i.e., before γ-secretase cleavage) were strongly expressed in tumor samples compared with controls (Figure 1B), whereas NOTCH2 expression was comparable in both groups (Figure 1B). Although the level of the transmembrane forms of NOTCH receptors does not reflect Notch activity, and NOTCH3 can be a direct target of NOTCH1 in some circumstances, this finding suggests that both NOTCH1 and NOTCH3 are mediators of the Notch pathway in EGFR-driven tumors *in vivo*.

To test whether Notch pathway activity is necessary for the growth of EGFR-driven tumors, we treated *EGFR*$^{T790M/L858R}$ mice with doxycycline for 8 weeks to induce tumor formation, and then randomly assigned them to three groups: i) control group, treated with vehicle and IgG antibody control; ii) GSI group, treated with dibenzazepine (DBZ), a potent and selective GSI; and iii) anti-NRR1/NRR3 group, treated with

blocking antibodies against NOTCH1 and NOTCH3, according to previously described treatment regimens (25-27). After five weeks of treatment, tumors represented more than 40% of the lung area in the control group, but only 20% and 10% in the DBZ and anti-NRR1/NRR3 groups, respectively (Figure 1C). This indicates that the Notch pathway is required for $EGFR^{T790M/L858R}$-driven tumor growth. Body weight was comparable in the three groups (Supplemental Figure 1A), suggesting the absence of the intestinal toxicity reported by other studies using regimens that led to stronger Notch inhibition (28).

As expected, analysis of protein expression by immunohistochemistry (IHC) of tumors from anti-NRR1/NRR3- or DBZ- treated mice showed fewer HES1-positive cells than in the vehicle-treated control group, implying that these treatments effectively inhibited the Notch pathway (Figure 1D). Moreover, the percentage of Ki67-positive cells was lower in tumors from the anti-NRR1/NRR3 and DBZ groups than the control group, indicating that Notch activity promotes cell proliferation in $EGFR^{T790M/L858R}$-driven tumors (Figure 1D). As the MAPK and AKT pathways are crucial downstream players of the EGFR signaling pathway (21), we also analyzed the expression of pERK and pAKT in the same samples. The percentage of pERK-positive cells was similarly reduced by treatment with the anti-NRR1 and -NRR3 antibodies and with DBZ compared control (Figure 1D), consistent with previous observations (13, 14). Conversely, the percentage of pAKT-positive cells was comparable in all groups (Supplemental Figure 1B).

Notch inhibition overcomes resistance to gefitinib in $EGFR^{T790M/L858R}$–driven lung adenocarcinoma

To study whether pharmacological inhibition of the Notch pathway *in vivo* had any impact on the resistance to gefitinib conferred by the gatekeeper mutation $EGFR^{T790M}$, we randomized $EGFR^{T790M/L858R}$ mice (after 8 weeks of doxycycline treatment) in four treatment groups: i) vehicle (control), ii) gefitinib, iii) DBZ, and iv) gefitinib + DBZ. For simplicity we decided to inhibit the Notch pathway hereafter only with a GSI.

As before, body weight was comparable in the different groups after the five weeks of treatment, suggesting that these drugs were well tolerated alone or in combination (Supplemental Figure 2A). In agreement with the previous findings (Figure 1C), tumor tissue occupied 42% of the lung in the control group, whereas it was decreased to 23% in the DBZ group (Figure 2A). As expected, gefitinib alone did not have any anti-tumor effect in $EGFR^{T790M/L858R}$ mice (52% of lung was tumor tissue). Conversely, the DBZ and gefitinib combination led to a very significant reduction of the tumor area compared with DBZ alone (tumor tissue covered only 10% of the total lung area) (Figure 2A).

Histopathological analysis of lung adenocarcinoma samples (i.e., non-benign tumors, Supplemental Figure 2B) showed that the single treatments had no effect on the lung adenocarcinoma number compared with control (i.e., vehicle-treated mice) (Figure 2B). Importantly, animals treated with the combination of gefitinib and Notch inhibition had significantly fewer lung adenocarcinomas than vehicle-treated ones (a mean of 10 lung adenocarcinoma per mouse *vs* 31 in the control, Figure 2B).

IHC analysis showed that the percentage of HES1-, Ki67-, pERK- and pAKT-positive cells was comparable in tumors from the gefitinib group and from controls (Figure 2C). By contrast, the percentage of HES1-, Ki67- and pERK-positive cells was reduced in tumors from DBZ-treated mice (Figure 2C), as before (Figure 1D), although in this case the difference was not significant for pERK. The percentage of HES1-,

Ki67- and pERK-positive cells tended to be lower in mice treated with the gefitinib and DBZ combination compared with DBZ-treated mice, particularly for pERK. Finally, the percentage of pAKT-positive cells was comparable in the DBZ, gefitinib and control groups, but interestingly, it was significantly reduced in the gefitinib + DBZ group compared with control mice (Figure 2C).

Altogether, these data demonstrate that inhibition of Notch signaling by DBZ restores sensitivity to treatment with gefitinib in $EGFR^{T790M/L858R}$-driven lung adenocarcinoma *in vivo*.

Notch inhibition overcomes resistance to gefitinib in lung adenocarcinoma patient-derived xenografts with $EGFR^{T790M/L858R}$ mutations

These results were very encouraging; however, it is considered that the best strategy for testing new cancer treatments is the combination of genetic mouse models and patient-derived xenograft (PDX) preclinical models (29). Therefore, we developed a lung adenocarcinoma PDX that harbors the $EGFR^{T790M/L858R}$ mutations, like our transgenic mouse model. One week after subcutaneous grafting of the PDX, nude mice were randomized in four groups as before: i) vehicle alone (control), ii) gefitinib, iii) DBZ, and iv) gefitinib + DBZ. Tumor growth was monitored for 30 days (i.e., the treatment duration). As expected, the $EGFR^{T790M}$ mutation conferred resistance to gefitinib. On the other hand, DBZ inhibited tumor growth, and strikingly, the DBZ and gefitinib combination almost totally blocked tumor growth (Figure 3A).

As before, IHC analysis of tumors showed that DBZ (alone or in combination with gefitinib) efficiently decreased the percentage of HES1-positive cells compared with control (Figure 3B). Tumor cell proliferation (Ki67-positive cells) was reduced by DBZ alone, and this effect was increased by addition of gefitinib. Similarly, the

percentage of pERK-positive cells was decreased by treatment with DBZ alone and even more by the DBZ and gefitinib combination compared with control. This indicated that the DBZ and gefitinib combination was more effective in reducing MAPK signaling than Notch inhibition alone. Finally, the percentage of pAKT-positive cells also was efficiently and similarly reduced by DBZ and by the DBZ and gefitinib combination.

Altogether, our results provide strong preclinical evidence for the likely therapeutic benefit of Notch inhibition and gefitinib combination in patients with TKI-resistant EGFR-driven lung adenocarcinoma harboring the gatekeeper mutation $EGFR^{T790M}$.

Combining EGFR TKIs and Notch inhibitors synergistically decreases HES1 expression

Our previous analysis showed that the DBZ and gefitinib combination is more efficient than each single treatment in reducing MAPK and AKT pathways. Previous reports, including work from our laboratory, identified HES1 as an important positive MAPK regulator in KRAS-driven lung adenocarcinoma (13, 30). Even more, HES1 has a similar effect on AKT signaling in T-cell acute lymphoblastic leukemia (T-ALL) (31). Therefore, we hypothesized that HES1 could be an important mediator of pERK and pAKT upon treatment with the DBZ and gefitinib combination. As the percentage of HES1-positive cells was similar in tumors from mice treated with DBZ alone and the DBZ and gefitinib combination in both preclinical models (Figure 2C and Figure 3B), we analyzed HES1 signal intensity in the same samples. Importantly, HES1 signal intensity was significantly lower in tumors from mice treated with the DBZ and

gefitinib combination than from mice treated with DBZ alone in the PDX model, and followed a similar trend in *EGFR*$^{T790M/L858R}$ mice (Figure 4, A and B).

To further validate our data, we analyzed HES1 expression by western blotting in PC9GR cells (previously used for the RNA-seq analysis, Figure 1A and Supplemental Table 1) after incubation with the different drugs alone or in combination. In accordance to our *in vivo* observation, HES1 expression was strongly reduced in cells exposed to the DBZ and gefitinib combination (Figure 4C).

Then, to explore HES1 role in PC9GR cells, we depleted HES1 using a pool of siRNAs targeting *HES1* mRNA (*siHES1*) (Supplemental Figure 3). Of note, proliferation of *siHES1*-treated cells was impaired compared with control cells transfected with the non-targeted siRNA (*siNT*), and this effect was potentiated in the presence of gefitinib (Figure 4D).

To test whether gefitinib effect was EGFR-mediated, we used the Chinese hamster ovary (CHO) cell line that is a natural null for EGFR, and was previously used for EGFR gain of function analyses (32). Interestingly, HES1 expression was not affected by co-treatment with DBZ and gefitinib in CHO cells transfected with empty vector, but was reduced in CHO cells that express EGFR$^{T790M/L858R}$ protein (Figure 4E). We concluded that EGFR is needed for HES1 expression reduction by the DBZ and gefitinib combination.

Taken together, our data indicate that the DBZ and gefitinib combination synergistically reduces the expression of HES1, a major driver in lung adenocarcinoma.

pSTAT3 directly binds to the *HES1* promoter and inhibits its expression

Previous studies have shown a benefit of combining EGFR TKIs and Notch inhibitors in TKI-sensitive cells, but the underlying mechanism was not fully described (15-17).

On the basis of the EGFR-dependent HES1 decrease in $EGFR^{T790M/L858R}$-expressing CHO cells upon incubation with the DBZ and gefitinib combination, we hypothesized that a common mechanism could be involved in the response to TKI treatment in TKI-sensitive and -resistant lung adenocarcinoma cells. An increase in the phosphorylation of STAT3 protein (pSTAT3), dependent on both JAK and FGFR activities, is reported in sensitive lung adenocarcinoma cells upon treatment with first-generation (erlotinib) and second-generation (afatinib) TKIs (33-35), hence, we investigated whether this occurred also in TKI-resistant cells.

Indeed, analysis of STAT3 phosphorylation status in PC9GR cells showed an increase in pSTAT3 levels upon gefitinib treatment (Figure 5A). This effect was partially inhibited by co-treatment with PD173074 or ruxolitinib, pan-inhibitors of FGFR and JAK pathways respectively. Even more, the combination of both inhibitors reduced pSTAT3 to levels lower than in control non-treated cells (Supplemental Figure 4). Moreover, we found that in the human *HES1* and mouse *Hes1* gene promoters, consensus binding sites for pSTAT3 (i.e., TTNNNNNAA) (36) are close to RBPJ sites (i.e., where the Notch transcription complex binds) (Supplemental Figure 5, A and B). To test whether pSTAT3 binds directly to the human *HES1* promoter in PC9GR cells, we performed chromatin immunoprecipitation (ChIP) experiments using antibodies against pSTAT3 and against NOTCH1, which is known to bind to the *HES1* promoter (positive control). NOTCH1 bound to the *HES1* promoter, and this interaction was reduced by incubation with DBZ (Figure 5B). Importantly, pSTAT3 bound to the *HES1* promoter only when cells were co-incubated with gefitinib and DBZ (Figure 5B). To determine whether pSTAT3 binding was critical for HES1 downregulation (Figure 4C), we incubated PC9GR cells with the various drug combinations after *siSTAT3* treatment that efficiently reduced both pSTAT3 and STAT3 expression (Figure 5C). Co-

incubation with gefitinib and DBZ strongly reduced HES1 protein level in control *siNT*-treated cells (Figure 5C), but strikingly, the same co-treatment kept HES1 levels in *siSTAT3*-treated cells (Figure 5C).

Altogether, these findings support that pSTAT3 decreases HES1 protein level by acting as a transcriptional repressor at the *HES1* promoter.

Notch inhibition overcomes resistance to osimertinib in human lung adenocarcinoma cells harboring the *EGFR* ^{C797S} mutation

As various TKIs increase pSTAT3 levels in lung adenocarcinoma cells (33-35), we asked whether the pSTAT3-dependent mechanism observed for gefitinib applied also to osimertinib. To this aim, we used the PC9GROR cell line (previously generated from PC9GR cells) that is resistant to osimertinib and harbor the gatekeeper mutation *EGFR*^{C797S} (18).

First, western blot analysis of PC9GROR cells incubated with DBZ and/or osimertinib showed that pSTAT3 levels increased upon osimertinib treatment. Accordingly, the combination of DBZ and osimertinib reduced HES1 protein levels (Figure 6A).

To test whether DBZ re-sensitized *EGFR*^{C797S} mutant human lung adenocarcinoma cells to osimertinib *in vivo*, we grafted PC9GROR cells subcutaneously in mice, and two weeks later, we treated them with DBZ and/or osimertinib for 3 weeks. Body weight remained comparable in the different treatment groups (Supplemental Figure 6A). Osimertinib alone had no significant effect on growth of PC9GROR cell xenografts (Figure 6B), while it strongly inhibited the growth of PC9GR xenografts (Supplemental Figure 6B). Similarly, DBZ showed no effect on growth of PC9GROR

cell xenografts, but importantly, tumor growth was strongly inhibited in mice treated with the osimertinib and DBZ combination (Figure 6B).

This finding demonstrates that treatment with DBZ restores sensitivity to osimertinib in human lung adenocarcinoma cells harboring the $EGFR^{C797S}$ mutation, confirming and extending our previous observations that DBZ sensitizes TKI-resistant tumors to TKIs.

Nirogacestat overcomes resistance to gefitinib in human lung adenocarcinoma cells harboring the $EGFR^{T790M}$ mutation

To strengthen the translational impact of our work, we wanted to confirm the Notch inhibitor sensitizing effect using a GSI under clinical trials. We chose nirogacestat because a recently finished phase 2 trial, showed that it has promising effects in patients with desmoid tumors, is well tolerated, and can be used for long-term treatments (37).

We randomized mice with subcutaneous PC9GR cell xenografts in six treatment groups: i) vehicle, ii) DBZ, iii) nirogacestat, iv) gefitinib, v) DBZ + gefitinib, vi) and nirogacestat + gefitinib. As gefitinib has some effect in PC9GR cells *in vitro* (Figure 4D), we used 10 mg/kg instead of the previously used dose of 20mg/kg. This lower concentration had a mild, non-significant effect on tumor growth compared with vehicle. Like in PC9GROR cells, the GSIs alone (DBZ and nirogacestat) did not have any effect. Conversely, gefitinib in combination with DBZ or nirogacestat strongly inhibited tumor growth (Figure 7A), as observed in mice harboring PDX and $EGFR^{T790M/L858R}$-driven tumors treated with the gefitinib and DBZ combination.

Moreover, Kaplan-Meier survival analysis of mice treated or not with nirogacestat and/or gefitinib showed that survival rate was comparable in mice treated

with vehicle, nirogacestat or gefitinib alone, although it tended to be higher in the gefitinib group (Figure 7B). By contrast, the nirogacestat with gefitinib combination increased survival compared with all other groups (median survival after treatment started: 24, 26.5, 32, and 39 days for vehicle, nirogacestat, gefitinib, and nirogacestat + gefitinib, respectively). For this analysis, we used only nirogacestat because at the used dose we could administer DBZ only for 5 weeks (26), while nirogacestat is well tolerated in patients for more than 2 years (37). As before, body weight was not significantly different in all groups during the experiment (Supplemental Figure 7).

These results show that the combination of gefitinib and nirogacestat increases the survival of mice xenografted with human lung adenocarcinoma cells that carry the $EGFR^{T790M}$ mutation conferring resistance to EGFR TKIs.

High HES1 protein levels correlate with poor progression-free survival and relapse in patients with EGFR mutated lung adenocarcinoma treated with TKIs

Our findings showed that HES1 has a key role in the resistance of EGFR-driven lung adenocarcinoma to TKI therapy. To strengthen this observation, we analyzed the correlation between progression-free survival (PFS) and nuclear HES1 protein levels in 75 patients with lung adenocarcinoma harboring *EGFR* mutations and treated with TKIs. We found that patients with low nuclear HES1 expression had a median PFS of 14 months, whereas patients with high nuclear HES1 expression had a median PFS of 7 months (hazard ratio 2.77, 95% CI [1.4-5.5], p = 0.006) (Figure 7C). Moreover, analysis of HES1 protein in tumor biopsy samples from patients with lung adenocarcinoma harboring *EGFR* activating mutations and treated with TKIs taken at diagnosis and after disease progression showed that HES1 nuclear levels were increased in samples

obtained at relapse in six of the seven patients ($p = 0.034$) (Figure 7D and Supplemental Figure 8).

These findings extend our previous study (14), and suggest a crucial role for HES1 in the relapse of patients with EGFR-driven lung adenocarcinoma under treatment with TKIs.

DISCUSSION

In this study, we confirmed and extended the observation that HES1 is a crucial mediator of the Notch pathway oncogenic activity in lung adenocarcinoma and uncovered its crucial role in resistance to EGFR TKIs.

We first observed that in mouse models of EGFR-driven lung adenocarcinoma, treatment with GSIs leads to decreased HES1 expression and pERK levels. This is consistent with studies in KRAS-driven lung adenocarcinoma mouse models showing that HES1-induced repression of DUSP1 increases pERK levels (13, 14). Therefore, we hypothesize that this is the same mechanism for the antitumor effect of Notch inhibitors when used as single treatment in EGFR-driven tumors.

Next, as a proof of concept of sensitizing cells with EGFR gatekeeper mutations to TKIs upon Notch inhibition, we found that murine and human EGFR-driven lung tumors harboring the $EGFR^{T790M}$ gatekeeper mutation sensitized to gefitinib when it is administered in combination with the GSI DBZ. Concomitantly, pAKT and pERK were further decreased upon combined treatment with gefitinib and DBZ, compared with the other treatments. It is known that HES1 represses PTEN and increases AKT activity in T-ALL (31), and represses DUSP1 and increases pERK levels in lung adenocarcinoma (30). Interestingly, we found in preclinical mouse models a higher HES1 decreased expression after treatment with the DBZ and gefitinib combination compared with DBZ alone. Moreover, HES1 loss of function sensitized human lung adenocarcinoma cells harboring the $EGFR^{T790M}$ mutation to gefitinib through a still unknown mechanism. In T-ALL, HES1 directly represses the *BBC3* gene that encodes PUMA, an inducer of apoptosis (38). Therefore, it is tempting to speculate that in lung adenocarcinoma cells, HES1 could repress *BBC3* or other genes encoding apoptosis-related factors, such as *BCL2L11* (i.e., BIM), crucial for gefitinib-induced cell death (39-41).

The $EGFR^{T790M}$ mutation does not totally inhibit gefitinib binding to EGFR (8, 9), and mutated EGFR is needed in CHO cells to reduce HES1 expression upon co-incubation with gefitinib and DBZ compared with DBZ alone. As the level of active, phosphorylated STAT3 is increased upon treatment with first- and second-generation TKIs (33-35), we hypothesized that this feature could explain the decreased levels of HES1 in our experimental setting. Indeed, incubation of $EGFR^{T790M}$ lung adenocarcinoma cells with gefitinib increased pSTAT3 levels in an FGFR- and JAK-dependent manner. Moreover, pSTAT3 directly interacted with the *HES1* promoter by ChIP analysis only when cells were gefitinib and DBZ co-treated. Finally, in PC9GR cells transfected with siRNAs against *STAT3*, HES1 levels were comparable in cells incubated with the combination of gefitinib and DBZ and with DBZ alone. These findings indicate that pSTAT3 represses HES1 expression effectively only when NOTCH processing is concomitantly inhibited, probably because the NOTCH transcriptional complex binds more efficiently to the *HES1* promoter than pSTAT3. A previous study showed that in sensitive EGFR-driven lung adenocarcinoma cells, erlotinib promotes Notch pathway induction after several days (16). We did not observe such induction, and this discrepancy could be due to the different treatment kinetics and/or the resistant background of PC9GR cells. Our data are in accordance with previous studies showing that pSTAT3 acts as a transcriptional repressor (42), and has a tumor suppressive role in prostate cancer (43), glioblastoma (44), and importantly, *KRAS*-driven lung adenocarcinoma (45). On the basis of these findings, the STAT3 inhibitors currently in clinical trials (46) should be used with caution, at least in tumors where the Notch pathway and consequently HES1 have a pro-tumorigenic role, as for instance in lung adenocarcinoma.

Our findings provided the proof of concept that lung adenocarcinoma cells with gatekeeper mutations conferring resistance to TKIs can be sensitized to such compounds by inhibiting the γ-secretase activity. To extend and validate our findings, we performed additional experiments using the lung adenocarcinoma PC9GROR cell line with the gatekeeper mutation $EGFR^{C797S}$ that confers resistance to the third-generation TKI osimertinib. The relevance of this experiment relies in results from a recent phase 3 clinical trial showing that the PFS of patients with EGFR mutated lung adenocarcinoma was significantly longer in the group with osimertinib as a first-line treatment than in the group with gefitinib or erlotinib (47). This might soon lead to the use of osimertinib as first-line treatment in patients with EGFR-mutated lung adenocarcinoma. Our data shows that osimertinib treatment in lung adenocarcinoma cells harboring the $EGFR^{C797S}$ mutation induced also pSTAT3 and when combined with DBZ further inhibited HES1 expression. Moreover, the DBZ and osimertinib combination strongly inhibited the growth of PC9GROR cell xenografts *in viv*o. This suggests that although osimertinib binding is highly reduced by the $EGFR^{C797S}$ gatekeeper mutation, it can still promote similar changes as observed in $EGFR^{T790M}$ cells treated with gefitinib. Moreover, these effects are exacerbated by Notch inhibition. Our results question the effect of the Notch pathway in the drug-tolerant state (48) in lung adenocarcinoma cells treated with osimertinib and this is currently an important area of study in the laboratory.

Overall, our new mechanistic findings highlight the role of HES1 in tumor relapse after EGFR TKI therapy. This was confirmed by the negative correlation between HES1 expression and PFS, as well as HES1 upregulation upon disease progression in patients with EGFR-mutated lung adenocarcinoma treated with TKIs. Our results are in agreement with a recent publication showing the negative correlation

between *HES1 mRNA* levels and PFS in a cohort of 64 patients with EGFR mutated non-small cell lung carcinoma treated with TKIs (49).

Our findings might be very relevant for patients with EGFR-driven lung adenocarcinoma that becomes resistant to osimertinib through acquisition of gatekeeper mutations, such as $EGFR^{C797S}$, and for whom treatment possibilities are limited to conventional therapies, because checkpoint inhibitors are mostly ineffective in this context. A phase 1 clinical trial should now be put in place to confirm the efficacy of the GSI–TKI combination in patients. Interestingly, a phase I/II trial in 16 patients with lung adenocarcinoma showed that the TKI erlotinib and GSI RO4929097 (Roche) combination is safe and feasible (50). As the side effects associated with erlotinib are higher than those with osimertinib (47), the osimertinib and GSI combination also might be safe in patients, particularly when using nirogacestat. Indeed, this GSI displays long-term efficacy and is well tolerated by patients (37). Moreover, the present study showed that similarly to DBZ, nirogacestat also overcomes resistance to TKIs in human lung adenocarcinoma cells harboring gatekeeper mutations.

MATERIAL AND METHODS

Mice

Tet-on-EGFR$^{T790M/L858R}$ and CCSP-rtTA mice were described previously (22, 23). For *in vivo* PC9GROR lung adenocarcinoma cell xenograft growth assays, 3.5 x 10^6 PC9GR or PC9GROR cells were injected subcutaneously in the flank of 6-week-old, female athymic Nude-Foxn1 mice (Envigo). Drug treatments were started when tumors reached the volume of 200 mm^3. For Kaplan-Meier analyses, mice were killed when tumors reached the volume of 1200 mm^3.

Animal procedures were performed according to protocols approved by the French national committee of animal care.

Western blotting

Western blotting was performed as previously described (14). The following antibodies were used for the analysis: anti-N1ICD, -HES1, -NOTCH1, -NOTCH2, -NOTCH3 and -pSTAT3 (Cell Signaling Technology), -STAT3 (BD), and -tubulin (Sigma). Secondary antibodies were horseradish peroxidase-linked anti-rabbit or anti-mouse (Cell Signaling Technology). Tubulin was used as loading control for all blots.

Treatments in mice

Dibenzazepine (DBZ) (Syncom) was administered 4 days per week (3.3 mg/kg/day) by intraperitoneal (IP) injection. Gefitinib and osimertinib (Cliniscience) were administered by gavage 4 days per week (20 mg/kg/day) and 5 days per week (5 mg/kg/day), respectively. Antibodies against NOTCH1 (NRR1) and NOTCH3 (NRR3) were administered by IP injection: NRR1 at 5 mg/kg/day every 5 days, and NRR3 at 15 mg/kg/day every Monday and Thursday (Genentech).

471

472 **Histopathology and immunohistochemistry**

473 Lung lobes were fixed, embedded in paraffin and stained with hematoxylin and eosin
474 (HE) or used for immunohistochemistry. Tumor area and total lung area were measured
475 using the Image J software. For pathological analysis of HE-stained tissue sections,
476 classical cytological and architectural features (tumor cell invasion and high mitotic
477 rate) were evaluated by our expert pathologist (M.C.). For immunohistochemistry, the
478 following antibodies were used: anti-HES1 (Cell Signaling Technology), -Ki67
479 (Agilent), -pERK (Cell Signaling Technology), and -pAKT (Novus Biologicals). For
480 each tumor, five 10X magnification fields were scored using the Image J software.
481 Signal intensity in murine and human tissue samples was scored as follows: 0 = lowest
482 intensity, and 5 = highest intensity.

483

484 **Cell culture and transfection reagents**

485 PC9GR (resistant to gefitinib), and PC9GROR (resistant to gefitinib and osimertinib)
486 cells were obtained from Yarden's laboratory (18). The control siRNA (non-targeting,
487 *siNT*), and the siRNAs against *HES1* (*siHES1*) and *STAT3* (*siSTAT3*) (Dharmacon) were
488 transfected at 20 nM with Dharmafect1 following the manufacturer's instructions.

489 For western blotting, RNA-seq or ChIP, cells were incubated with DBZ (250
490 nM), gefitinib (1 μM), osimertinib (250 nM), PD173074 (2μM), ruxolitinib (0.25 μM),
491 or DMSO (vehicle).

492 For the proliferation assays, siRNA-transfected cells were incubated with
493 gefitinib (15 nM) (or DMSO). Then, cells were fixed at various time points and stained
494 with sulforhodamine B (SRB). Absorbance was measured at 560 nm in a microplate
495 reader (Glomax, Promega).

RNA sequencing

RNA was sequenced by Fasteris (Switzerland) using Next-Generation DNA sequencing (NGS) based on the Illumina technology. The RNA-seq data were deposited in the National Center for Biotechnology Information Gene Expression Omnibus (accession number GSE117846).

Reads were aligned against the Ensembl *Homo sapiens* genome assembly (GRCh38). Read counts were extracted from the STAR output file with HTSeq and only the protein-coding genome features were taken into account in the final count matrix. Sample counts were normalized by summing read counts for each sample ($s_i, i = 1, \dots, 12$), and computing a first factor for each sample $f_i = s_i / \text{median}_{j=1,\dots,12}(s_j)$. These factors were normalized such that the product of all the normalized factors g_i was equal to 1: $g_i = \frac{f_i}{\sqrt[1/12]{\prod_{j=1,\dots,12} f_j}}$. Finally, each column (each sample) of the read count matrix was divided by the corresponding g_i. Gene set enrichment analysis (19) was performed using «The Molecular Signatures Database Hallmark Gene Set Collection» (20).

Chromatin immunoprecipitation (ChIP)

Chromatin was prepared as described previously (51). The ChIP-Adem-Kit and ChIP DNA Prep Adem-Kit (Ademtech) were used for ChIP and DNA purification, respectively, on an AutoMag robot, according to the manufacturer's instructions. The anti-NOTCH1 antibody was purchased from Abcam and the anti-pSTAT3 antibody from Cell Signaling Technology.

519 The immunoprecipitated DNA was analyzed by PCR using the following
520 primers:
521 Prom*HES1* Fw: GAAGGCAATTTTTCCTTTTTC
522 Prom*HES1* Rev: AAGTTCCCGCTCAGACTTTAC
523

524 **Patient-derived xenograft model**

525 The patient-derived xenograft (PDX) was generated in Paz-Ares's laboratory at the
526 Instituto de Biomedicina de Sevilla (IBIS). The lung adenocarcinoma was classified
527 (TNM) as T2a N1 M0. A tumor piece of 0.5 mm^3 was implanted in the right flank of
528 mice, and after two weeks, mice were randomized for treatment.
529

530 **Patients and ethical considerations**

531 Tumors were analyzed from 75 patients with lung adenocarcinoma harboring EGFR
532 mutations and treated with EGFR TKIs at Toulouse University Hospital (52). Four
533 patients were included in the MOSCATO (NCT01566019) or MATCH-R
534 (NCT02517892) clinical trials at the Institut Gustave Roussy, Paris. All patients signed
535 an informed consent form to allow tissue analyses. This study was approved by the
536 Committee for the Protection of Persons of each institution, and by the French National
537 Agency for Medicines and Health Products Safety (ANSM).
538

539 **Statistical analysis**

540 Unless otherwise specified, data are presented as mean ± S.E.M. One way analysis of
541 variance (ANOVA) was carried out to assess the significance of the different expression
542 levels in IHC, and to determine differences in tumor growth and body weight among
543 animal groups. Correlation of HES1 expression in patient samples and PFS, and

544 Kaplan-Meier survival curves were analyzed with the Gehan–Breslow–Wilcoxon test.
545 Hazard ratios were calculated with the Mantel-Haenszel test. Samples (cells or mice)
546 were allocated to their experimental group according to their pre-determined type (cell
547 type or mouse treatment). Investigators were blinded to the experimental groups for the
548 analysis of data presented in Figures 1C, 1D, 2A, 2B, 2C, 3A, 3B, 4A, 4B, 5D, 7C and
549 7D. For the rest they were not blinded.
550 # $p \leq 0.1$; * $p \leq 0.05$; ** $p \leq 0.01$; *** $p \leq 0.001$, **** $p \leq 0.0001$.

ACKNOWLEDGMENTS

We thank Daniel Herranz, Laurent Le Cam, Daniel Fisher, Hélène Tourriere, and Manuel Serrano for helpful discussion and critical reading of the manuscript. Elisabetta Andermarcher professionally edited the manuscript. We thank Dom Helmlinger for technical help with the RNA-seq. We thank the IRCM animal facility members for their outstanding work. We thank the Cell Signaling Technology immunohistochemistry technical service for their help. E.B. was supported by a contract from *Fondation de France*. S.B. was supported by a fellowship from the French Ministry of Education and Research. M.M. is supported by a contract from *Fondation ARC*. Work in A.M.'s lab is supported by the *Fondation ARC* (PJA 20131200405), the European Commission (CIG631431), the *Institute de Cancer de Montpellier Fondation*, and the *Institut National du Cancer* (INCa_9257 and INCa-DGOS-Inserm 6045). The funders had no role in study design, data collection and analysis, decision to publish, or preparation of the manuscript. E.B. designed and performed most experiments, analyzed data and wrote the manuscript. S.B. performed the RNA-seq experiments and, together with L.P., performed some experiments. M.M. M.G. and A.G. performed some *in vivo* treatments. E.F. performed the ChIP experiments. I.F., and L.P-A designed and performed the PDX experiments. X.Q., J-L. P., O.C., J-C. S., J.M. and G.F. performed experiments on clinical samples. M.C. performed the immunohistochemistry analysis of mouse tumors. H.P.M and E.C. supervised the experiments with STAT3. Y.G. and N.P. performed some IHC experiments. K-K.W. supervised the experiments in $EGFR^{T790M/L858R}$ mice. A.T. and J.C. performed the RNA-seq analysis. C.S. supervised the experiments with the anti-NRR1 and NRR3 antibodies. A.M. designed and supervised the study, secured funding, analyzed data, and wrote the manuscript. All authors discussed the results and commented the manuscript.

FIGURES

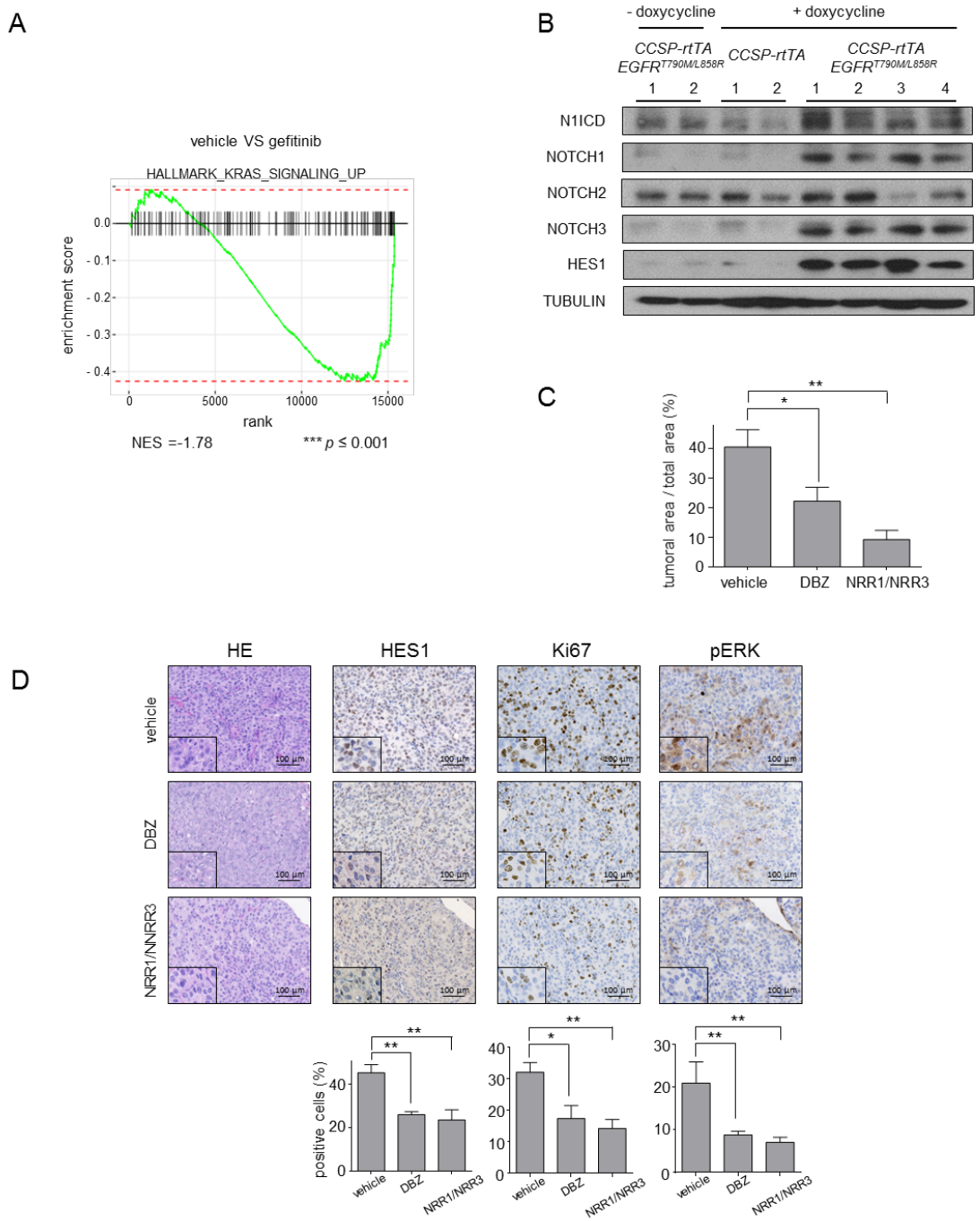

Figure. 1. Inhibition of Notch signaling hampers tumor growth in *EGFR*$^{T790M/L858R}$ mice.

(A) PC9GR cells were starved for 18h and then treated with vehicle (DMSO) or gefitinib (1 µM) for 6h. RNA was extracted from cells and subjected to RNAseq. The KRAS-associated Gene Set was downregulated in PC9GR cells treated with gefitinib

compared with control (n = 3 per condition; FDR < 0.001). **(B)** Immunoblotting of the indicated proteins in lungs from control mice (four lanes on the left) and in mice with $EGFR^{T790M/L858R}$-driven tumors (four lanes on the right). Controls were littermates of $EGFR^{T790M/L858R}$ mice without doxycycline induction or *CCSP-rtTA* mice treated with doxycycline. **(C)** The tumor area relative to the total lung area in mice with $EGFR^{T790M/L858R}$-driven tumors treated with methocel and IgG (vehicle; n = 6), with a γ-secretase inhibitor (DBZ; n = 6), or with anti-NOTCH1 and anti-NOTCH3 antibodies (NRR1/NRR3; n = 5) was determined by staining tissue sections with hematoxylin and eosin (H&E). **(D)** H&E and immunohistochemical staining of lung tumor sections from the same mice as in **C**. The histograms show the staining quantification (percentage of positive cells) in the corresponding sections obtained by analysis of 5 fields (10X) per tumor. Values correspond to the mean ± SEM; Statistical significance was determined by a one-way ANOVA test: * $p \leq 0.05$, ** $p \leq 0.01$

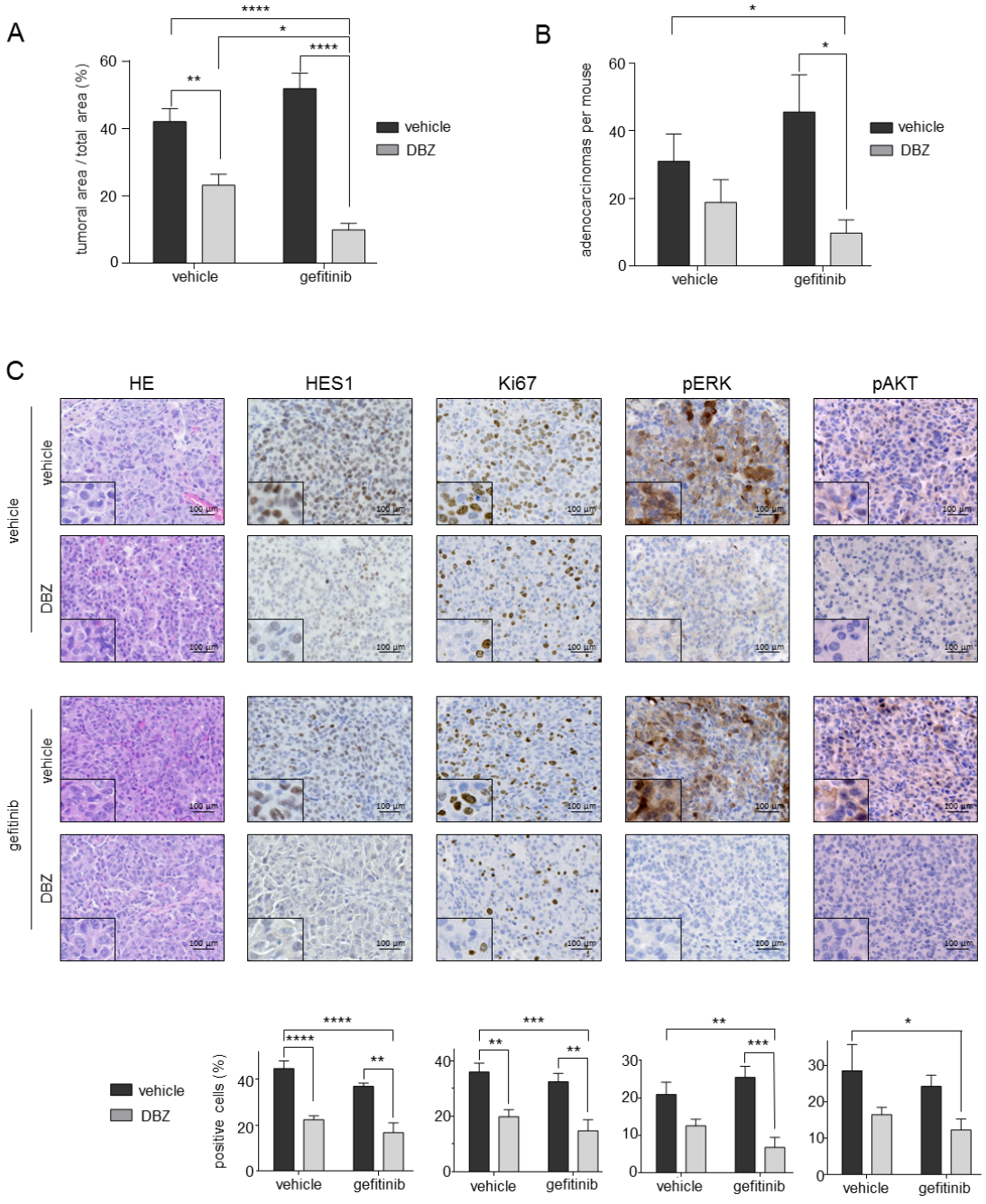

Figure. 2. Notch inhibition overcomes resistance to gefitinib in mouse *EGFR $^{T790M/L858R}$*-driven tumors.

(A) The tumor area relative to the total lung area in lung tissue sections from mice with *EGFR*$^{T790M/L858R}$-driven tumors treated with methocel (vehicle; n = 9), DBZ (n = 10), gefitinib (n = 7), or the DBZ and gefitinib combination (n = 8) was determined by staining tissue sections with H&E. **(B)** Number of lung adenocarcinomas in the mice

described in **A**. **(C)** H&E and immunohistochemical staining of tumors from the mice described in **A**. The histograms show the percentage of positive cells in the corresponding sections obtained by analysis of 5 fields (10X) per tumor. Values correspond to the mean ± SEM. Statistical significance was determined by a one-way ANOVA test: * $p \leq 0.05$, ** $p \leq 0.01$, *** $p \leq 0.001$ and **** $p \leq 0.0001$. In panel 2A, the comparison between gefitinib and DBZ single treatments was significant (****). In panel 2C, HES1 and pERK expression levels in tumors after treatment with gefitinib alone and DBZ alone also were significantly different (* and **, respectively).

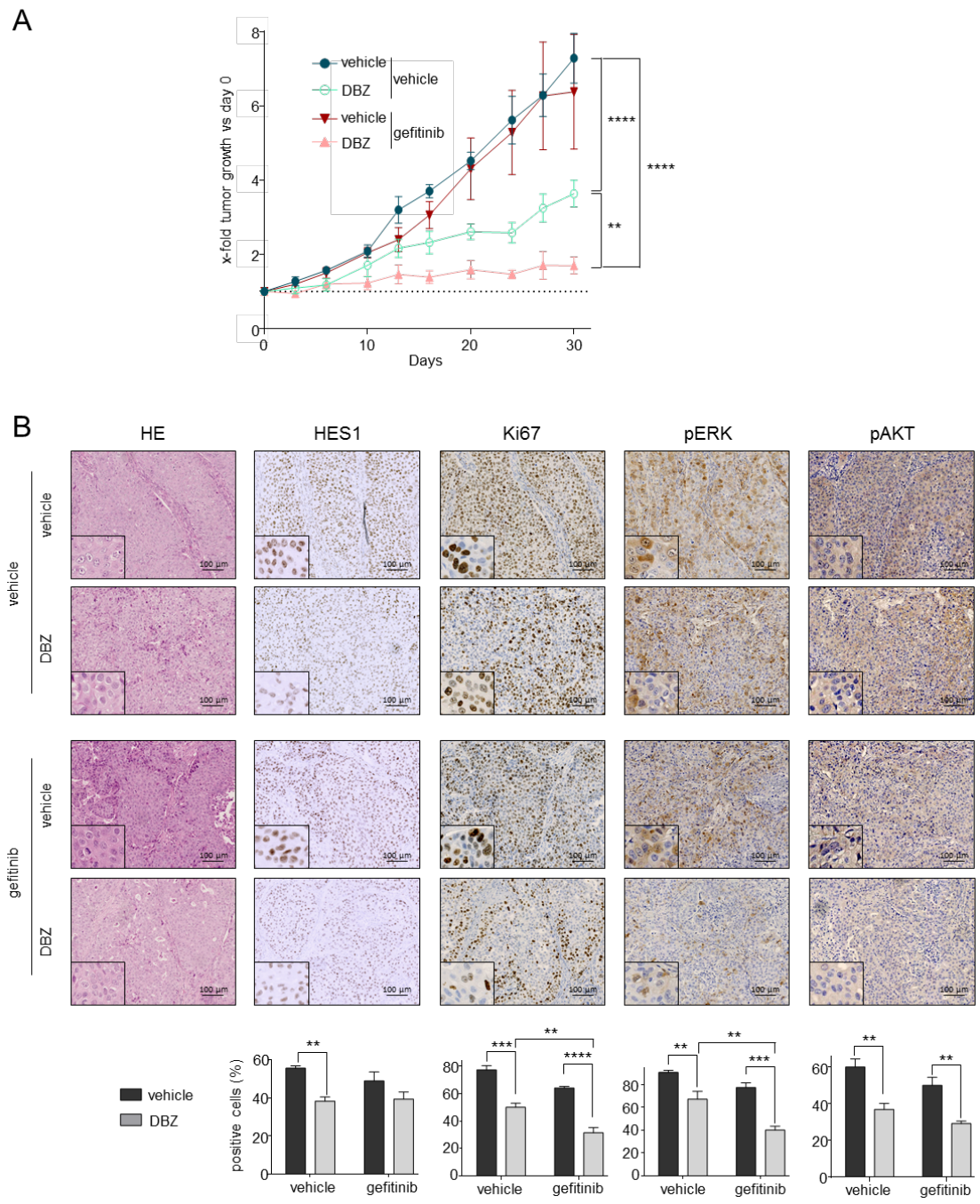

Figure. 3. Notch inhibition overcomes resistance to gefitinib in human *EGFR*$^{T790M/L858R}$-driven lung adenocarcinoma.

(A) Growth of *EGFR*$^{T790M/L858R}$ lung adenocarcinoma PDX implanted in the right flank of nude mice. When tumors were approximately 100 mm^3 in volume, mice were treated with vehicle (methocel, n = 5), DBZ (n = 5), gefitinib (n = 4), or the DBZ and gefitinib combination (n = 5). The y-axis shows the fold-increase in tumor size versus day 0. **(B)**

H&E and immunohistochemical staining of tumor sections from the mice described in **A**. The histograms show the percentage of positive cells in the corresponding sections. For each treatment, 5 fields (10X) per mouse were analyzed. Values correspond to the mean ± SEM. Statistical significance was determined by two-way ANOVA in A, and one-way ANOVA in B: * $p \leq 0.05$, ** $p \leq 0.01$, *** $p \leq 0.001$ and **** $p \leq 0.0001$. In panel 3A, the comparisons between gefitinib and DBZ single treatments and between gefitinib and the combination were also significant (*** and ****, respectively). In panel 3B, the comparison between vehicle and DBZ was also significant for all analyses (** for HES1 and **** for Ki67, pERK and pAKT), as well as the comparison between gefitinib and DBZ for Ki67 expression (*).

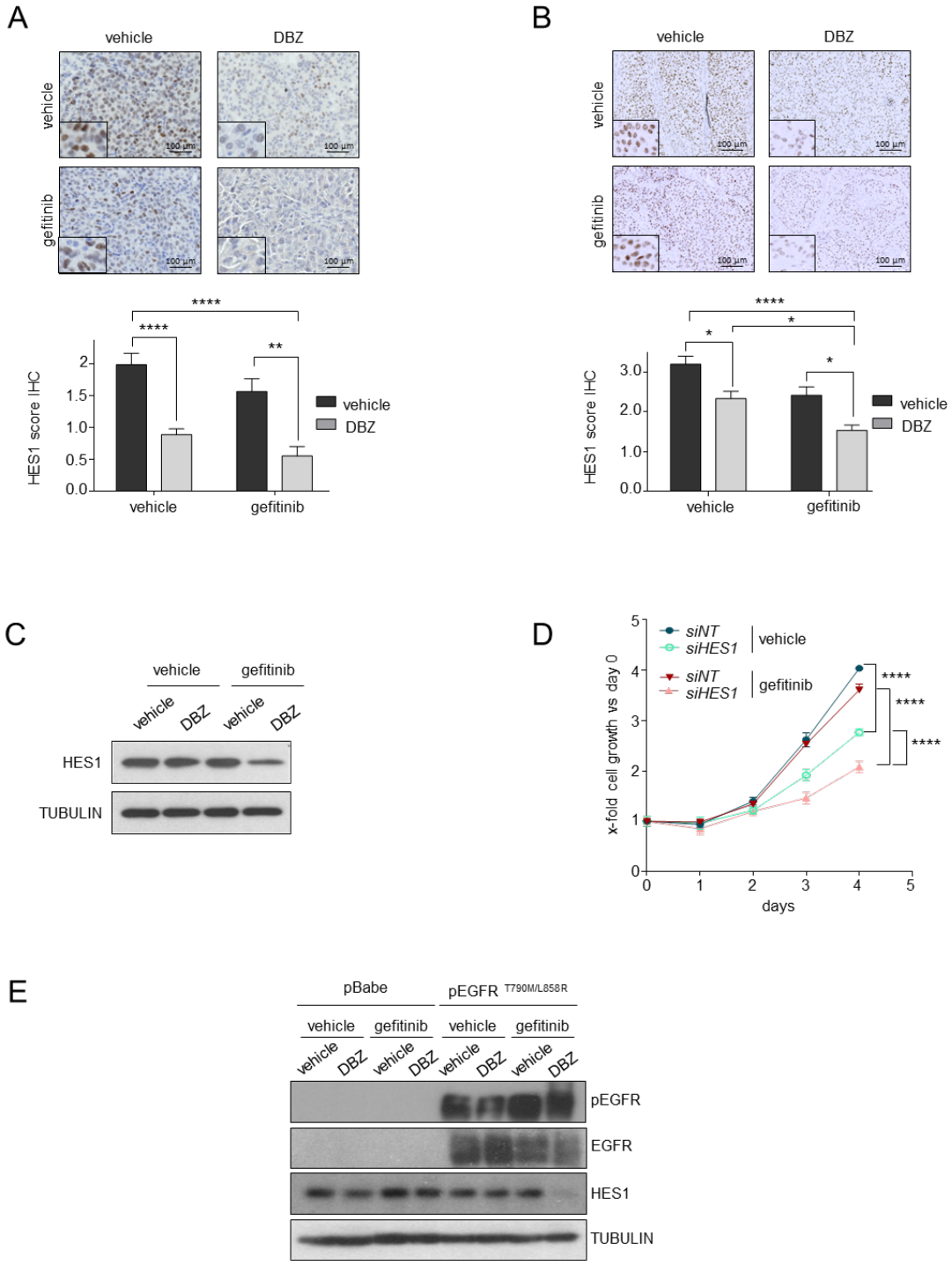

Figure. 4. Combining EGFR TKIs and Notch inhibitors synergistically decreases HES1 expression.

(A) Immunohistochemical analysis of HES1 expression in tumors from *EGFR*$^{T790M/L858R}$ mice treated with methocel (vehicle; n = 9), DBZ (n = 10), gefitinib (n = 7), or the DBZ and gefitinib combination (n = 8). The histograms show the quantification of HES1

signal intensity by analysis of 5 tumor fields (10X) per mouse. **(B)** Immunohistochemical analysis of HES1 expression in tumors from *EGFR*$^{T790M/L858R}$ PDX implanted in nude mice treated with vehicle (methocel, n = 5), DBZ (n = 5), gefitinib (n = 4), or the combination (n = 5). **(C)** Immunoblotting of the indicated proteins in PC9GR cells treated with vehicle (DMSO), DBZ (250 nM) or/and gefitinib (1 μM). **(D)** Proliferation of PC9GR cells transfected with a non-targeting siRNA (*siNT*) or against *HES1* (*siHES1*) and treated with vehicle (DMSO) or gefitinib (15 nM) for 72 h. Data are the mean ± SEM (n = 3 in all groups). **(E)** Immunoblotting of the indicated proteins in control (pBabe vector) and in EGFR$^{T790M/L858R}$ protein expressing CHO cells treated with vehicle (DMSO), DBZ (250 nM) and/or gefitinib (1 μM). This is a representative image of two different experiments.

Values correspond to the mean ± SEM. Statistical significance was evaluated with the one-way ANOVA test in A and B, and the two-way ANOVA test in D: * $p \leq 0.05$, ** $p \leq 0.01$, *** $p \leq 0.001$ and **** $p \leq 0.0001$. In panel 4A, the comparison between gefitinib alone and DBZ alone was also significant (*). In panel 4B, the comparison between vehicle and gefitinib was also significant (*). In panel 4D, the comparisons between *siNT*/vehicle and *siNT*/gefitinib, between *siNT*/vehicle and *siHES1*/gefitinib, and between *siNT*/gefitinib and *siHES1*/gefitinib also were significant (**, ****, and ****, respectively).

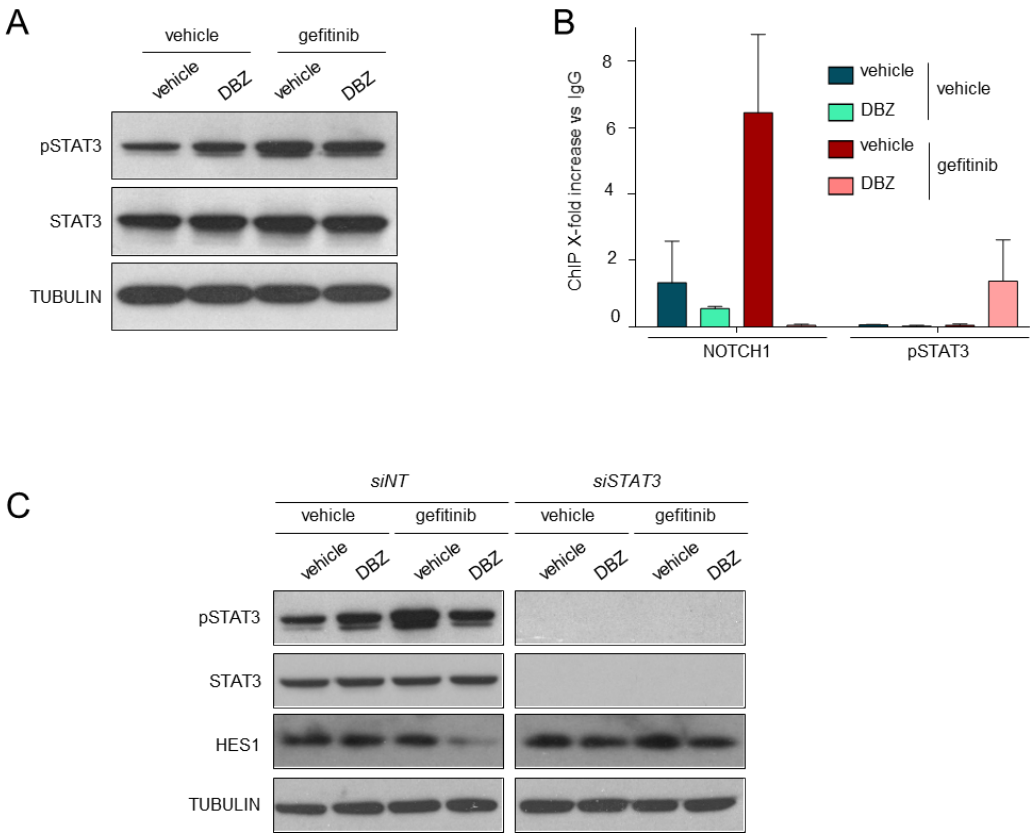

Figure. 5. pSTAT3 directly binds to the *HES1* promoter and inhibits its expression. **(A)** Immunoblotting of the indicated proteins in PC9GR cells treated with vehicle (DMSO), DBZ (250 nM) and/or gefitinib (1 µM). **(B)** ChIP analysis of NOTCH1 and pSTAT3 binding to the *HES1* promoter in PC9GR cells treated as in **A**. **(C)** Immunoblotting of the indicated proteins in PC9GR cells transfected with a non-targeting siRNA (*siNT*) or against *STAT3* (*siSTAT3*) and treated with vehicle (DMSO), DBZ (250 nM) and/or gefitinib (1 µM).

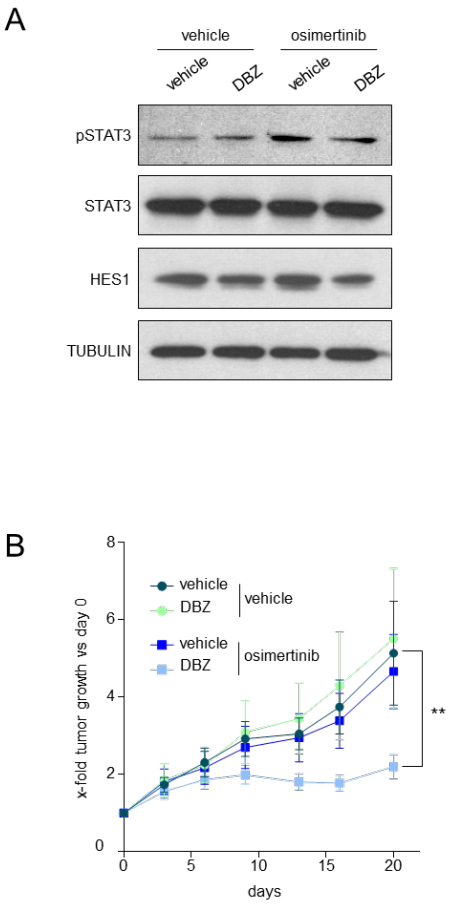

Figure. 6. Notch inhibition overcomes resistance to osimertinib in *EGFR*^{C797S} human lung adenocarcinoma cells.

(A) Immunoblotting of the indicated proteins in PC9GROR cells treated with vehicle (DMSO), DBZ (250 nM) and/or osimertinib (250 nM). **(B)** Nude mice xenografted with PC9GROR cells (subcutaneous injection in the right flank) were treated with vehicle (methocel, n = 8), DBZ (n = 8), osimertinib (n = 8), or the DBZ and osimertinib combination (n = 7). The y-axis shows the tumor growth fold increase versus day 0. Values correspond to the mean ± SEM. Statistical significance was determined by two-

way ANOVA test: * $p \leq 0.05$, ** $p \leq 0.01$, *** $p \leq 0.001$ and **** $p \leq 0.0001$. In panel 6B, the comparisons between DBZ alone and the combination, and between osimertinib and the combination also were significant (** and *, respectively).

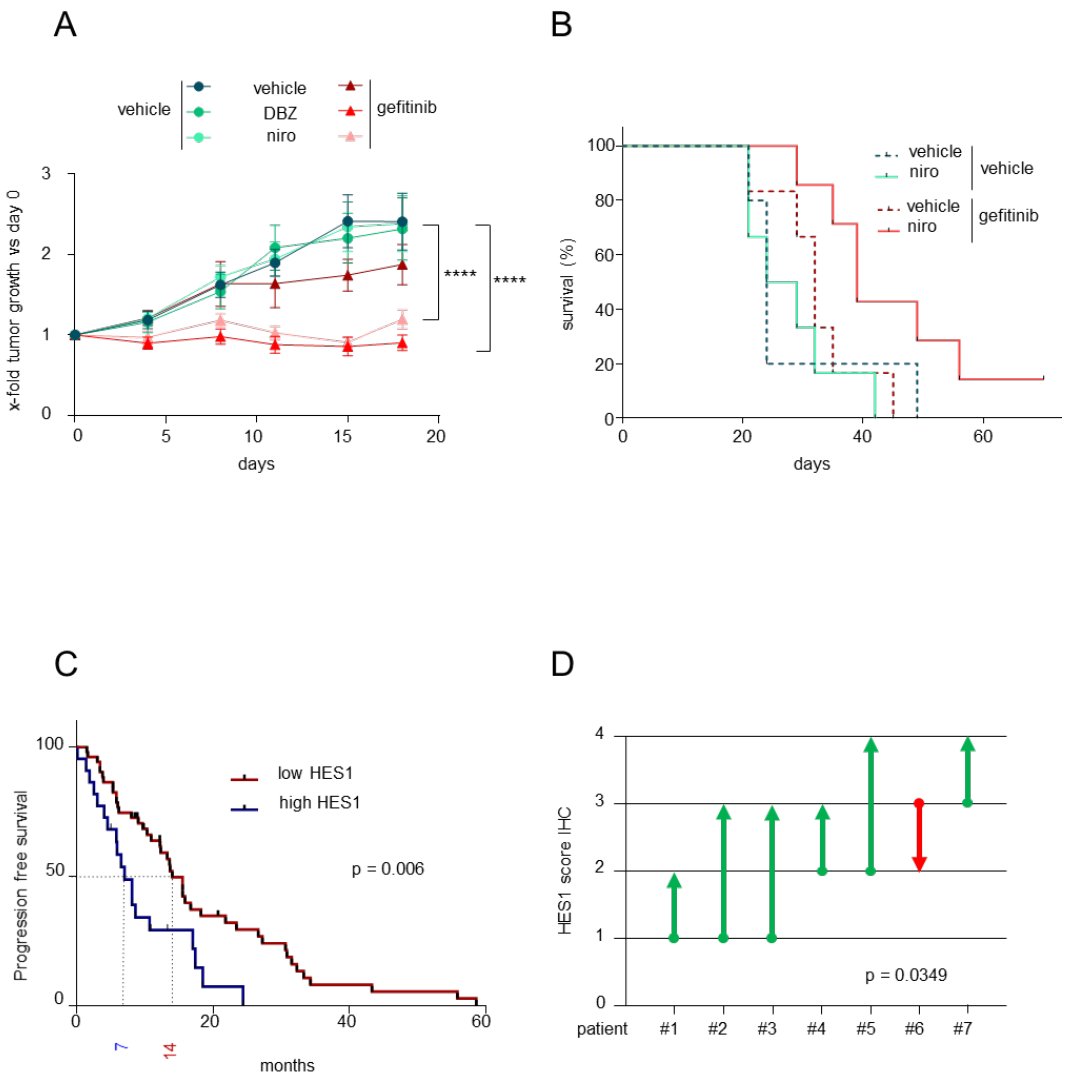

Figure. 7. High HES1 protein levels correlate with poor progression-free survival and relapse in patients with EGFR-mutated lung adenocarcinoma treated with TKIs.

(A) Nude mice were xenografted with PC9GR cells and then treated with vehicle (methocel, n = 6), DBZ (n = 6), nirogacestat (n = 6), gefitinib (n = 6), the DBZ and gefitinib combination (n = 7), or the nirogacestat and gefitinib combination (n = 7). The y-axis shows the tumor growth fold increase versus day 0. Values correspond to the mean ± SEM. Statistical significance was determined by a two-way ANOVA test: * p ≤

0.05, ** $p \leq 0.01$, *** $p \leq 0.001$ and **** $p \leq 0.0001$. The comparisons between DBZ and the DBZ-gefitinib combination and between DBZ and the nirogacestat-gefitinib combination also were significant (**** and ***, respectively), as well as the comparison between nirogacestat and the DBZ-gefitinib or the nirogacestat-gefitinib combination (**** and ****, respectively) and the comparison between gefitinib and the DBZ-gefitinib combination (**). **(B)** Nude mice were xenografted with PC9GR cells and then treated with vehicle (methocel, n = 5), nirogacestat (n = 6), gefitinib (n = 6), or the nirogacestat+gefitinib combination. Statistical significance was determined by Gehan–Breslow–Wilcoxon test: vehicle *vs* gefitinib (p = 0.3), vehicle *vs* nirogacestat (p = 0.93), vehicle *vs* the combination (p = 0.021), gefitinib *vs* the combination (p = 0.05), and nirogacestat vs the combination (p = 0.02). **(C)** Progression-free survival of EGFR TKI-treated patients with *EGFR*-mutated lung adenocarcinoma (n = 75) classified according to the tumor HES1 expression assessed by IHC staining (low HES1 = 0–2.50 HES1 score; high HES1 = 2.51–5.00 HES1 score). Statistical significance was determined with the Gehan–Breslow–Wilcoxon test. **(D)** Representation of HES1 staining intensity score change in tumor samples from seven patients with *EGFR*-mutated lung adenocarcinoma before TKI treatment (dot) and after relapse (arrowhead). Statistical significance was determined with the paired two-tailed Student's *t* test.

REFERENCES

1. Herbst RS, Heymach JV, and Lippman SM. Lung cancer. *N Engl J Med.* 2008;359(13):1367-80.
2. Rosell R, Bivona TG, and Karachaliou N. Genetics and biomarkers in personalisation of lung cancer treatment. *Lancet.* 2013;382(9893):720-31.
3. Reck M, Heigener DF, Mok T, Soria JC, and Rabe KF. Management of non-small-cell lung cancer: recent developments. *Lancet.* 2013;382(9893):709-19.
4. Tan CS, Gilligan D, and Pacey S. Treatment approaches for EGFR-inhibitor-resistant patients with non-small-cell lung cancer. *Lancet Oncol.* 2015;16(9):e447-59.
5. Janne PA, Yang JC, Kim DW, Planchard D, Ohe Y, Ramalingam SS, et al. AZD9291 in EGFR inhibitor-resistant non-small-cell lung cancer. *N Engl J Med.* 2015;372(18):1689-99.
6. Thress KS, Paweletz CP, Felip E, Cho BC, Stetson D, Dougherty B, et al. Acquired EGFR C797S mutation mediates resistance to AZD9291 in non-small cell lung cancer harboring EGFR T790M. *Nat Med.* 2015;21(6):560-2.
7. Le X, Puri S, Negrao MV, Nilsson M, Robichaux JP, Boyle TA, et al. Landscape of EGFR -dependent and -independent resistance mechanisms to osimertinib and continuation therapy post-progression in EGFR-mutant NSCLC. *Clin Cancer Res.* 2018.
8. Yun CH, Mengwasser KE, Toms AV, Woo MS, Greulich H, Wong KK, et al. The T790M mutation in EGFR kinase causes drug resistance by increasing the affinity for ATP. *Proc Natl Acad Sci U S A.* 2008;105(6):2070-5.
9. Yoshikawa S, Kukimoto-Niino M, Parker L, Handa N, Terada T, Fujimoto T, et al. Structural basis for the altered drug sensitivities of non-small cell lung cancer-associated mutants of human epidermal growth factor receptor. *Oncogene.* 2013;32(1):27-38.
10. Bray SJ. Notch signalling in context. *Nat Rev Mol Cell Biol.* 2016;17(11):722-35.
11. Takebe N, Miele L, Harris PJ, Jeong W, Bando H, Kahn M, et al. Targeting Notch, Hedgehog, and Wnt pathways in cancer stem cells: clinical update. *Nat Rev Clin Oncol.* 2015;12(8):445-64.
12. Licciulli S, Avila JL, Hanlon L, Troutman S, Cesaroni M, Kota S, et al. Notch1 is required for Kras-induced lung adenocarcinoma and controls tumor cell survival via p53. *Cancer Res.* 2013;73(19):5974-84.
13. Baumgart A, Mazur PK, Anton M, Rudelius M, Schwamborn K, Feuchtinger A, et al. Opposing role of Notch1 and Notch2 in a Kras-driven murine non-small cell lung cancer model. *Oncogene.* 2014.
14. Maraver A, Fernandez-Marcos PJ, Herranz D, Canamero M, Munoz-Martin M, Gomez-Lopez G, et al. Therapeutic Effect of gamma-Secretase Inhibition in Kras(G12V)-Driven Non-Small Cell Lung Carcinoma by Derepression of DUSP1 and Inhibition of ERK. *Cancer Cell.* 2012;22(2):222-34.
15. Konishi J, Yi F, Chen X, Vo H, Carbone DP, and Dang TP. Notch3 cooperates with the EGFR pathway to modulate apoptosis through the induction of bim. *Oncogene.* 2010;29(4):589-96.
16. Arasada RR, Amann JM, Rahman MA, Huppert SS, and Carbone DP. EGFR blockade enriches for lung cancer stem-like cells through Notch3-dependent signaling. *Cancer Res.* 2014;74(19):5572-84.

17. Hu S, Fu W, Li T, Yuan Q, Wang F, Lv G, et al. Antagonism of EGFR and Notch limits resistance to EGFR inhibitors and radiation by decreasing tumor-initiating cell frequency. *Sci Transl Med.* 2017;9(380).
18. Mancini M, Gal H, Gaborit N, Mazzeo L, Romaniello D, Salame TM, et al. An oligoclonal antibody durably overcomes resistance of lung cancer to third-generation EGFR inhibitors. *EMBO Mol Med.* 2018;10(2):294-308.
19. Subramanian A, Tamayo P, Mootha VK, Mukherjee S, Ebert BL, Gillette MA, et al. Gene set enrichment analysis: A knowledge-based approach for interpreting genome-wide expression profiles. *Proceedings of the National Academy of Sciences.* 2005;102(43):15545-50.
20. Liberzon A, Birger C, Thorvaldsdottir H, Ghandi M, Mesirov JP, and Tamayo P. The Molecular Signatures Database (MSigDB) hallmark gene set collection. *Cell Syst.* 2015;1(6):417-25.
21. Arteaga CL, and Engelman JA. ERBB receptors: from oncogene discovery to basic science to mechanism-based cancer therapeutics. *Cancer Cell.* 2014;25(3):282-303.
22. Li D, Shimamura T, Ji H, Chen L, Haringsma HJ, McNamara K, et al. Bronchial and peripheral murine lung carcinomas induced by T790M-L858R mutant EGFR respond to HKI-272 and rapamycin combination therapy. *Cancer Cell.* 2007;12(1):81-93.
23. Tichelaar JW, Lu W, and Whitsett JA. Conditional expression of fibroblast growth factor-7 in the developing and mature lung. *J Biol Chem.* 2000;275(16):11858-64.
24. Zheng Y, de la Cruz CC, Sayles LC, Alleyne-Chin C, Vaka D, Knaak TD, et al. A rare population of CD24(+)ITGB4(+)Notch(hi) cells drives tumor propagation in NSCLC and requires Notch3 for self-renewal. *Cancer Cell.* 2013;24(1):59-74.
25. Choy L, Hagenbeek TJ, Solon M, French D, Finkle D, Shelton A, et al. Constitutive NOTCH3 Signaling Promotes the Growth of Basal Breast Cancers. *Cancer Res.* 2017;77(6):1439-52.
26. Rivera-Torres J, Guzman-Martinez G, Villa-Bellosta R, Orbe J, Gonzalez-Gomez C, Serrano M, et al. Targeting gamma-secretases protect against angiotensin II-induced cardiac hypertrophy. *J Hypertens.* 2015;33(4):843-50.
27. Wu Y, Cain-Hom C, Choy L, Hagenbeek TJ, de Leon GP, Chen Y, et al. Therapeutic antibody targeting of individual Notch receptors. *Nature.* 2010;464(7291):1052-7.
28. van Es JH, van Gijn ME, Riccio O, van den Born M, Vooijs M, Begthel H, et al. Notch/gamma-secretase inhibition turns proliferative cells in intestinal crypts and adenomas into goblet cells. *Nature.* 2005;435(7044):959-63.
29. Day CP, Merlino G, and Van Dyke T. Preclinical mouse cancer models: a maze of opportunities and challenges. *Cell.* 2015;163(1):39-53.
30. Maraver A, and Serrano M. Notching up a new therapeutic strategy for Non-Small Cell Lung Carcinoma (NSCLC). *Oncotarget.* 2012.
31. Palomero T, Sulis ML, Cortina M, Real PJ, Barnes K, Ciofani M, et al. Mutational loss of PTEN induces resistance to NOTCH1 inhibition in T-cell leukemia. *Nat Med.* 2007;13(10):1203-10.
32. Lo HW, Hsu SC, Ali-Seyed M, Gunduz M, Xia W, Wei Y, et al. Nuclear interaction of EGFR and STAT3 in the activation of the iNOS/NO pathway. *Cancer Cell.* 2005;7(6):575-89.

33. Kim SM, Kwon OJ, Hong YK, Kim JH, Solca F, Ha SJ, et al. Activation of IL-6R/JAK1/STAT3 signaling induces de novo resistance to irreversible EGFR inhibitors in non-small cell lung cancer with T790M resistance mutation. *Mol Cancer Ther.* 2012;11(10):2254-64.
34. Lee HJ, Zhuang G, Cao Y, Du P, Kim HJ, and Settleman J. Drug resistance via feedback activation of Stat3 in oncogene-addicted cancer cells. *Cancer Cell.* 2014;26(2):207-21.
35. Codony-Servat C, Codony-Servat J, Karachaliou N, Molina MA, Chaib I, Ramirez JL, et al. Activation of signal transducer and activator of transcription 3 (STAT3) signaling in EGFR mutant non-small-cell lung cancer (NSCLC). *Oncotarget.* 2017;8(29):47305-16.
36. Darnell JE, Jr. STATs and gene regulation. *Science.* 1997;277(5332):1630-5.
37. Kummar S, O'Sullivan Coyne G, Do KT, Turkbey B, Meltzer PS, Polley E, et al. Clinical Activity of the gamma-Secretase Inhibitor PF-03084014 in Adults With Desmoid Tumors (Aggressive Fibromatosis). *J Clin Oncol.* 2017;35(14):1561-9.
38. Schnell SA, Ambesi-Impiombato A, Sanchez-Martin M, Belver L, Xu L, Qin Y, et al. Therapeutic targeting of HES1 transcriptional programs in T-ALL. *Blood.* 2015;125(18):2806-14.
39. Gong Y, Somwar R, Politi K, Balak M, Chmielecki J, Jiang X, et al. Induction of BIM Is Essential for Apoptosis Triggered by EGFR Kinase Inhibitors in Mutant EGFR-Dependent Lung Adenocarcinomas. *PLOS Medicine.* 2007;4(10):e294.
40. Costa DB, Halmos B, Kumar A, Schumer ST, Huberman MS, Boggon TJ, et al. BIM Mediates EGFR Tyrosine Kinase Inhibitor-Induced Apoptosis in Lung Cancers with Oncogenic EGFR Mutations. *PLOS Medicine.* 2007;4(10):e315.
41. Cragg MS, Kuroda J, Puthalakath H, Huang DCS, and Strasser A. Gefitinib-Induced Killing of NSCLC Cell Lines Expressing Mutant EGFR Requires BIM and Can Be Enhanced by BH3 Mimetics. *PLOS Medicine.* 2007;4(10):e316.
42. Zhang H, Hu H, Greeley N, Jin J, Matthews AJ, Ohashi E, et al. STAT3 restrains RANK- and TLR4-mediated signalling by suppressing expression of the E2 ubiquitin-conjugating enzyme Ubc13. *Nat Commun.* 2014;5:5798.
43. Pencik J, Schlederer M, Gruber W, Unger C, Walker SM, Chalaris A, et al. STAT3 regulated ARF expression suppresses prostate cancer metastasis. *Nat Commun.* 2015;6:7736.
44. Peixoto P, Blomme A, Costanza B, Ronca R, Rezzola S, Palacios AP, et al. HDAC7 inhibition resets STAT3 tumorigenic activity in human glioblastoma independently of EGFR and PTEN: new opportunities for selected targeted therapies. *Oncogene.* 2016;35(34):4481-94.
45. Grabner B, Schramek D, Mueller KM, Moll HP, Svinka J, Hoffmann T, et al. Disruption of STAT3 signalling promotes KRAS-induced lung tumorigenesis. *Nat Commun.* 2015;6:6285.
46. Johnson DE, O'Keefe RA, and Grandis JR. Targeting the IL-6/JAK/STAT3 signalling axis in cancer. *Nat Rev Clin Oncol.* 2018;15(4):234-48.
47. Soria JC, Ohe Y, Vansteenkiste J, Reungwetwattana T, Chewaskulyong B, Lee KH, et al. Osimertinib in Untreated EGFR-Mutated Advanced Non-Small-Cell Lung Cancer. *N Engl J Med.* 2018;378(2):113-25.
48. Sharma SV, Lee DY, Li B, Quinlan MP, Takahashi F, Maheswaran S, et al. A chromatin-mediated reversible drug-tolerant state in cancer cell subpopulations. *Cell.* 2010;141(1):69-80.

49. Codony-Servat J, Codony-Servat C, Cardona AF, Gimenez-Capitan A, Drozdowskyj A, Berenguer J, et al. Cancer Stem Cell Biomarkers in EGFR-Mutation-Positive Non-Small-Cell Lung Cancer. *Clin Lung Cancer.* 2019;20(3):167-77.
50. Gold KA, Byers LA, Fan YH, Fujimoto J, Tse WH, Lee JJ, et al. A phase I/II trial combining erlotinib with gamma secretase inhibitor RO4929097 in advanced non-small cell lung cancer (NSCLC). *Journal of Clinical Oncology.* 2013;31(15_suppl):8104-.
51. Fabbrizio E, El Messaoudi S, Polanowska J, Paul C, Cook JR, Lee JH, et al. Negative regulation of transcription by the type II arginine methyltransferase PRMT5. *EMBO Rep.* 2002;3(7):641-5.
52. Calvayrac O, Mazieres J, Figarol S, Marty-Detraves C, Raymond-Letron I, Bousquet E, et al. The RAS-related GTPase RHOB confers resistance to EGFR-tyrosine kinase inhibitors in non-small-cell lung cancer via an AKT-dependent mechanism. *EMBO Mol Med.* 2017;9(2):238-50.